ChemPubSoc Europe

DOI: 10.1002/chem.201500811

CHEMISTRY
A European Journal
Full Paper

Structure Elucidation

The Structure and Conformation of $(CH_3)_3CSNO$

Antonela Canneva,[a] Mauricio F. Erben,[a] Rosana M. Romano,[a] Yury V. Vishnevskiy,[b] Christian G. Reuter,[b] Norbert W. Mitzel,[b] and Carlos O. Della Védova*[a]

Abstract: The gas-phase molecular structure of $(CH_3)_3CSNO$ was investigated by using electron diffraction, allowing the first experimental geometrical parameters for an *S*-nitrosothiol species to be elucidated. Depending on the orientation of the –SNO group, two conformers (*anti* and *syn*) are identified in the vapor of $(CH_3)_3CSNO$ at room temperature, the *syn* conformer being less abundant. The conformational landscape is further scrutinized by using vibrational spectroscopy techniques, including gas-phase and matrix-isolation IR spectroscopy, resulting in a contribution of ca. 80:20 for the *anti*:*syn* abundance ratio, in good agreement with the computed value at the MP2(full)/cc-pVTZ level of approximation. The UV/Vis and resonance Raman spectra also show the occurrence of the conformational equilibrium in the liquid phase, with a moderate post-resonance Raman signature associated with the 350 nm electronic absorption.

The nitric oxide molecule, NO, behaves as a free radical and is important in inorganic and organic chemistry, in basic research and industry, pharmacy, biochemistry, neuroscience, physiology, and immunology. It was declared "Molecule of the Year" in 1992.[1] In biochemical terms it can be produced through the metabolism of L-arginine by nitric oxide synthases (NOS). An important role of NO is the production of cyclic guanosine monophosphate (cGMP). Another significant function is its irreversible reaction with thiols to produce *S*-nitrosothiols, RSNO (also called thionitrites). They are less stable than the bond-isomeric N-sulfinylimines, RNSO, and were first recognized as early as 1840 as reported by Oae and Shinhama.[2] To date more than 1000 proteins involving *S*-nitrosothiols have been reported. Closely related with the evolution, it has been suggested that the blood concentration of NO in humans depends on the altitude of their habitation.[3] Both the incremented NOS activity to produce NO and the release of NO from *S*-nitrosothiols are the consequences of sojourn at high altitude that enhances hypoxia tolerance. This helps rationalize the evolutionary result of elevated NO concentrations in the blood of Tibetan highlanders due to acclimatization over long periods of time. Thus the importance of the *S*-nitrosothiols is indisputable. Closely related to these results is a depletion of the concentration of airway *S*-nitrosothiols in individuals with asthma.[4]

Therefore, and also due to the not-less-important property as light-sensitive compounds, converting them into NO donor drugs[5,6] and their atmospheric implications,[7] a wide range of spectroscopic and analytical methods has been applied in all of these studies.[8]

S-Nitrosothiols, RSNO, are often highly reactive species, and the isolation of pure substances has been attained only in a few cases. Accordingly, structural studies are scarce and many fundamental properties of this class of compounds remain poorly understood. In view of the high importance of this family of compounds, a gas-phase structural determination of an simple model RSNO exponent remained desirable. Herein we report a detailed spectroscopic characterization of $(CH_3)_3CSNO$ and present its gas-phase structure determined by electron diffraction, including conformational analysis. The latter is important in relation to the biological properties of this kind of compound. The bond isomers, the *N*-sulfinylimines RNSO, show an unique *syn* configuration.[9]

Two conformers are expected for RSNO compounds depending on the orientation of the R–S single bond with respect to the N=O group. These forms are denoted *syn* and *anti* describing the mutual orientation of the S–R single and N=O double bonds (Scheme 1).

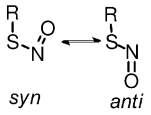

Scheme 1. Conformational equilibrium around the S–N bond in *S*-nitrosothiols.

Based on steric hindrance considerations, it was assumed that tertiary RSNO compounds prefer the *anti* conformation and primary and secondary ones the *syn* conformation. The first crystal structure of an *S*-nitrosothiol confirmed this: *S*-nitroso-*N*-acetyl-DL-penicillamine (2-acetamido-3 methyl-3-thionitrosobutanoic acid) adopts an *anti*

[a] *Dr. A. Canneva, Prof. Dr. M. F. Erben, Prof. Dr. R. M. Romano, Prof. Dr. C. O. Della Védova*
Departamento de Química, Facultad de Ciencias Exactas
Universidad Nacional de La Plata, CC962
CEQUINOR (UNLP-CONICET, CCT, La Plata)
La Plata (CP 1900) (República Argentina)
E-mail: carlosdv@quimica.unlp.edu.ar

[b] *Dr. Y. V. Vishnevskiy, C. G. Reuter, Prof. Dr. N. W. Mitzel*
Universität Bielefeld
Lehrstuhl für Anorganische Chemie und Strukturchemie
Centrum für Molekulare Materialien CM2
Universitätsstrasse 25, 33615 Bielefeld (Germany)

Supporting information for this article is available on the WWW under http://dx.doi.org/10.1002/chem.201500811.

conformation in the crystal.[10] The crystal structure of triphenyl thionitrite by Arulsami et al. also contains molecules with an *anti* conformation (τ(CS–NO) = 175.7°),[11] whereas the primary *S*-nitrosocaptopril thionitrite adopts a *syn* conformation (τ(CS–NO) = 0.7°) in its crystals.[12,13] A few other crystal structures have been reported.[14] However, it becomes apparent that other than steric effects, in particular electronic properties of the group R determine the conformational preference.[15] For instance, the preference for an *anti* conformation of the primary CF_3SNO thionitrite[16] has been attributed to the electron withdrawing nature of the CF_3 group. Thus, a delicate balance between steric, mesomeric, and inductive effects should be expected to affect the conformational behavior. Notably, for the bond isomeric *N*-sulfinylimines, the example PhNSO shows a *syn* configuration for its –N=S=O group, and this is maintained even upon introduction of two ethyl groups in *ortho* positions of the phenyl ring. Thus, the configuration transferability is assured by rotation of the –N=S=O group by 55.3° from the former planar arrangement and the *syn* configuration around the N=S bond is retained.[17]

Controversies remain on the nature of the S–N bonds in RSNO compounds. On one hand, quite high rotation barriers are observed for the *syn*→*anti* interconversion, suggesting a partial S–N double-bond character. On the other hand, the computed homolytic dissociation energy, typically 30 kcal mol^{-1},[18] suggests that this bond is relatively weak. A balance between two different electronic effects has been suggested: 1) delocalization of the p-type lone pair formally located on the sulfur atom into the π^*(NO) orbital imparts a partial double-bond character to the S–N bond and explains the tendency for planarity of the CSNO group; and 2) the hyperconjugative interaction between the p-type lone pair at oxygen and the σ^*(SN) orbital contrarily weakens the S–N bond.[19] The contribution of an ionic resonance structure can be considered based on the corresponding NO stretching frequency. It is known that the N–O bond order increases with contribution of an NO^+ ionic character and this is favored by electronegative substituents attached to the NO group.[20] We have recently demonstrated that the ν(N=O) stretching mode can be also used as a sensor for the determination of conformational properties in RSNO compounds in the gas phase.[21] The N=O fundamental stretching vibration usually differs by several wavenumber units for the *syn* and *anti* conformations and the absorptions appear in a comparatively uncrowded region of the IR spectrum at about 1550 cm^{-1}.[22]

The determination of the structure of an *S*-nitrosothiol as a free molecule in the gas phase becomes mandatory to shed more precise information on these issues. The conformational properties of $(CH_3)_3CSNO$ were previously studied by variable-temperature ^{15}N NMR spectroscopy in [D_8]toluene solution; a *anti/syn* relationship of 4.78:1 was measured at 298 K.[11] Moreover, quantum-chemical calculations at the MP2/6-311+G(2df) level of approximation suggest that the *anti* form is preferred for a free molecule by ca. 1.0 kcal mol^{-1}.[15] A comprehensive study about families of X–Y–NO species (with Y = C, N, O, S) has been also reported.[23] Both rotamers of $(CH_3)_3CSNO$, *anti* and *syn* (Figure 1), were found to be stable minima on the potential energy surface for the internal rotation about N–S and S–C bonds at the B3LYP/cc-pVTZ level of theory (Figure 2). The dominance of the *anti* over the *syn* conformer has been estimated with energy differences of 0.87 and 0.85 kcal mol^{-1} at the B3LYP/cc-pVTZ and MP2(full)/cc-pVTZ levels of theory, respectively.

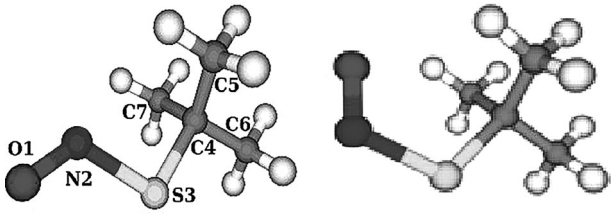

Figure 1. Molecular structures and atom numbering (excluding hydrogen atoms) of *anti* (left) and *syn* conformers (right) of $(CH_3)_3CSNO$. For complete atom numbering, see the Supporting Information, Figure S1.

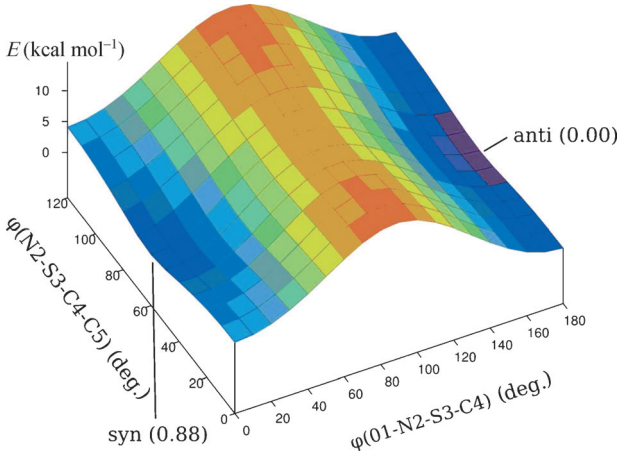

Figure 2. Potential-energy surface and relative energy values of *anti* and *syn* conformers of $(CH_3)_3CSNO$ calculated on the B3LYP/cc-pVTZ level.

Figure 3 depicts the gas-phase electron diffraction (GED) experimental and best-model radial distribution curves of $(CH_3)_3CSNO$. To describe the conformational behavior of $(CH_3)_3CSNO$ by means of GED, the following models have been evaluated. The one-conformer models for the *anti* and *syn* conformers gave total structural R_{str} factors of 7.0 and 12.3%, respectively. The refinement of a two-conformer model consisting of a mixture of the *anti* and *syn* conformations gave the best agreement with the experimental intensities (R_{str} = 6.2%) for a ratio 79(8)% *anti*. The refined structure parameters of $(CH_3)_3CSNO$ are collected in Table 1. The largest correlation in the least squares refinement (−0.85) was between the *r*(N–O) bond length and the scale factor for the first group of amplitudes (Supporting Information, Table S6). All other correlations were below 0.7. Table 2 contains a number of relevant solid-state structural and conformational parameters for SNO containing compounds, which are compared with our gas-phase structural values.

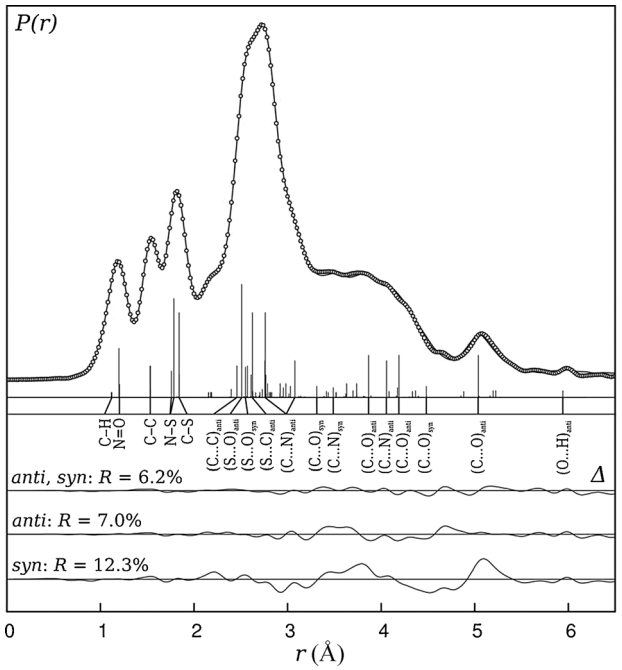

Figure 3. Experimental (○) and best model (——) radial distribution curves of $(CH_3)_3CSNO$. Difference curves for different models are shown beneath.

The gas-phase IR spectrum of $(CH_3)_3CSNO$ is interpreted regarding their conformational properties. It would be interesting to analyze the behavior of the ν(N=O) stretching vibration to infer differences in the force constant for this mode. The IR spectrum shows an intense A-band absorption centered at 1534 cm^{-1} ($\Delta PR = 12\ cm^{-1}$), which can be assigned with confidence to the ν(N=O) fundamental mode of vibration of the more stable *anti* conformer, since the N=O oscillator vibrates almost parallel with respect to the *A* principal axis of inertia of the molecule. Interestingly, superimposed to this strong absorption at lower energies, a less intense but not so clear B band at 1513 cm^{-1} ($\Delta(PQ-QR) = 9\ cm^{-1}$) can be distinguished. The 1600–1400 cm^{-1} region of the IR spectrum of $(CH_3)_3CSNO$ is shown in Figure 4. Harmonic frequency calculations for the *syn* and *anti* conformers of $(CH_3)_3CSNO$ reproduce this spectrum. In effect, the ν(N=O) frequency values for *anti* and *syn* conformers are computed to be 1488 and 1454 cm^{-1}, respectively, at the MP2(full)/cc-pVTZ level of approximation.

To ensure and take advantage of these conformational features, FTIR spectra of the sample isolated in an Ar matrix have been recorded and its photochemical behavior subsequently analyzed (Figure 5).

The FTIR Ar-matrix spectrum shows the presence of two clear absorptions at 1514 and 1494 cm^{-1}, which are assigned to the *anti* and *syn* rotamers, respectively. A relative increase in the intensity of the band at 1494 cm^{-1} at the expense of the most intense band at 1514 cm^{-1} with the increase of the UV/

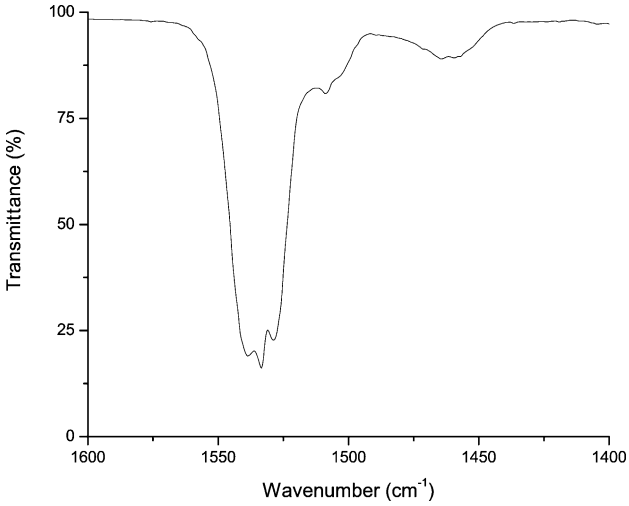

Figure 4. Gas-phase FTIR spectrum of $(CH_3)_3CSNO$ in the N=O stretching fundamental region.

Table 1. Experimental and theoretical bond lengths [Å] and angles [°] of $(CH_3)_3CSNO$ (esd given as 3σ).

	anti			*syn*		
	Experimental[a]		Calculated[b]	Experimental[a]		Calculated[b]
Parameter	r_g	r_e[c]		r_g	r_e[c]	
r(N=O)	1.199(5)	1.195(5)[1]	1.207	1.205(5)	1.202(5)[1]	1.214
r(S–N)	1.787(2)	1.770(2)[2]	1.775	1.761(2)	1.744(2)[2]	1.750
r(C–S)	1.842(2)	1.828(2)[2]	1.833	1.844(2)	1.829(2)[2]	1.834
r(C4–C5)	1.531(2)	1.520(2)[3]	1.524	1.533(2)	1.521(2)[3]	1.525
r(C4–C6)	1.534(2)	1.522(2)[3]	1.526	1.536(2)	1.524(2)[3]	1.528
$r(C–H)_{av}$	1.124(5)	1.103(5)[4]	1.090	1.124(5)	1.102(5)[4]	1.089
∢(O-*N*-S)	–	113.6(6)[5]	114.9	–	117.3(6)[5]	118.6
∢(N-S-C)	–	97.6(14)[6]	96.9	–	109.3(14)[6]	108.6
∢(S-C-C5)	–	109.5(4)[7]	110.0	–	109.9(4)[7]	110.5
∢(S-C-C6)	–	102.2(8)[8]	104.8	–	101.3(8)[8]	103.9
$∢(C4-C-H)_{av}$	–	109.5(8)[9]	110.3	–	109.5(8)[9]	110.3
∢(C5-C4-C6)	–	114.3(12)[d]	110.4	–	102.8(25)[a]	109.9
∢(C5-C4-C7)	–	107.0(19)[d]	111.1	–	126.4(41)[a]	111.9
φ(N-S-C-C5)	–	58.5(11)[10]	61.3	–	71.7(29)[11]	62.2
χ [%]	79(8)		86[e]	21(8)		14[e]

[a] GED. [b] MP2(full)/cc-pVTZ. [c] 1,2,…10 refer to groups of parameters; the differences between values of parameters in each group were fixed on MP2(full)/cc-pVTZ values.[d] dependent parameter. [e] calculated from theoretical ΔG° values for the temperature of experiment (277 K).

Table 2. Structural and conformational parameters for *S*-nitrosothiol-containing compounds determined by X-ray crystallography (esd given as 1σ) compared to the structure of $(CH_3)_3CSNO$ determined in the gas phase by electron diffraction herein (esd given as 3σ).

	Conformation	*r*(C–S) [Å]	*r*(S–N) [Å]	*r*(N=O) [Å]	∢(SNO) [°]	∢(CSN) [°]	Φ(CSNO) [°]	Ref.
$(CH_3)_3CSNO$	*anti* (79%)	1.828(2)	1.770(2)	1.195(5)	113.6(6)	97.6(14)	*anti*	–
	syn (21%)	1.829(2)	1.744(2)	1.205(5)	117.3(6)	109.3(14)	*syn*	
2-(acetylamino)-2-carboxy-1,1-dimethylethyl thionitrite	*anti*	1.841(3)	1.771(3)	1.214(4)	113.2(2)	100.4(1)	–	[24]
	–	–	–	–	–	–	–	
2-acetamido-3 methyl-3-thionitrosobutanoic acid	*anti*	1.833(1)	1.763(2)	1.199(2)	113.99(11)	100.80(7)	176.3	[13]
	–	–	–	–	–	–	–	
$ONSC(Me)_2CH_2NHC(O)Me$	*anti*	1.829(2)	1.754(2)	1.206(2)	114.9(2)	94.44(8)	178.5	[25]
Ph_3CSNO	*anti*	1.867(3)	1.792(5)	1.177(6)	114.0(4)	102.1(2)	175.7	[14]
Tri(3,5-bis(2,6-dimethylphenyl)phenyl-SNO	*anti* (67%)	1.841(4)	1.781(5)	1.205(6)	111.4(6)	104.2(3)	179.6	[26]
	syn (33%)	1.841(4)	1.781(5)	1.189(12)	123.6(7)	104.2(3)	7.3	[26]
S-nitrosocaptopril[a]	*syn*	1.800	1.766	1.206	117.7	103.7	0.68	[12]
S-nitroso-L-cysteine ethyl ester hydrochloride	*syn* molec. A	1.734(2)	1.769(3)	1.191(4)	117.6(2)	105.6(1)	2.4(3)	[16]
	syn molec. B	1.638(2)	1.728(5)	1.183(7)	116.4(4)	109.5(2)	3.3(5)	[16]

[a] Accuracy is not reported by the authors.

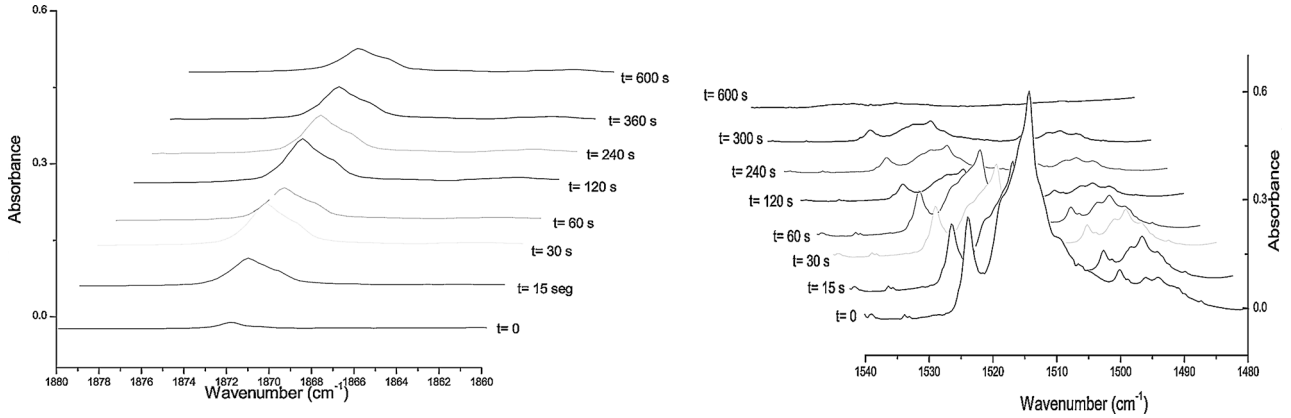

Figure 5. FTIR spectra of an Ar matrix containing $(CH_3)_3CSNO$ in the 1880–1860 and 1540–1480 cm^{-1} region immediately after deposition ($t=0$) and after the indicated broad band UV/Vis irradiation times.

Vis broad band irradiation time becomes apparent. This photoisomerization behavior is common to other reported systems and implies a randomization process. First, the system reaches an excited electronic state, and subsequently decays with almost the same probability in the ground electronic state of each rotamer.[27] The intensity ratio of the two non-irradiated N=O bands is roughly 0.17:1 and agrees within experimental error with the abundance ratio between the *syn* and the most stable *anti* form (0.27(10):1), as determined experimentally by GED. Therefore the ν(N=O) IR intensity absorption coefficient of the *anti* conformer is 1.6 times higher than that of the *syn* form. The data in Figure 5 confirm that after 6 min of UV/Vis broad band irradiation, the system reaches about equal abundance of *syn* and *anti* rotamers. Again a factor of 1.6 is estimated experimentally. This agrees also with the end in the NO production clearly identified by the occurrence of a new band at 1872 cm^{-1}, the intensity of which seems to decrease with prolonged irradiation (Figure 5). This fact may be related with its photo degradation and also with the formation of NO byproducts explicable by NO mobility even under cryogenic experimental conditions.[28] Longer irradiation leads to the complete photolysis of the title molecule. Although it is commonly accepted that *S*-nitrosothiols decompose under formation of the corresponding disulfides and NO by a unimolecular homolytic scission of the S–N bond,[29] there is no clear indication to the formation of the $(CH_3)_3CSNO^{\bullet}$ radical[28] in our matrix spectra. Further studies are being conducting to better understand the photochemical behavior of the title molecule isolated in an inert matrix environment.

As earlier recognized,[30] the measurement of Raman spectra for *S*-thionitrites is a very difficult task because the compounds decompose under laser irradiation. The Raman spectrum of $(CH_3)_3CSNO$ has been successfully measured with 1064 nm excitatio, maintaining the laser output power as low as possible. Moreover, the typical green color adopted by the sample invites to explore its resonance Raman (RR) effect with visible light lasers. These spectra elegantly complement the gas-phase and matrix-isolation IR spectra, allowing for a complete description of the vibrational properties of the title species. The main features associated with conformational behavior will be discussed herein. Thus, Figure 6 depicts the normalized RR spectra of $(CH_3)_3CSNO$ in the N=O stretching fundamental

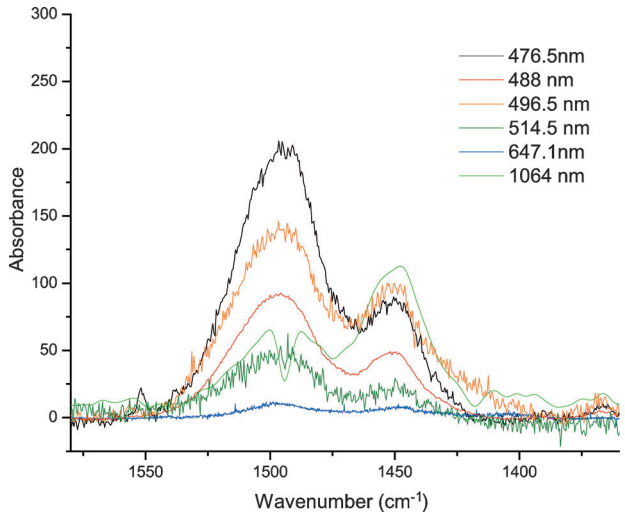

Figure 6. Normalized RR spectra of $(CH_3)_3CSNO$ in the N=O stretching fundamental region.

region. The maximum ν(N=O) band intensity of the normalized spectra against the lower wavenumber normal mode of vibration of 153 cm^{-1} was reached, when the highest energy excitation used in our experiments (laser at 476.5 nm) was applied. In the Figure 7 the normalized resonance Raman spectra of liquid $(CH_3)_3CSNO$ in the region 850–500 cm^{-1}, the Raman spectra of liquid $(CH_3)_3CSSC(CH_3)_3$, and matrix IR spectra of $(CH_3)_3CSNO$ are included for comparison.

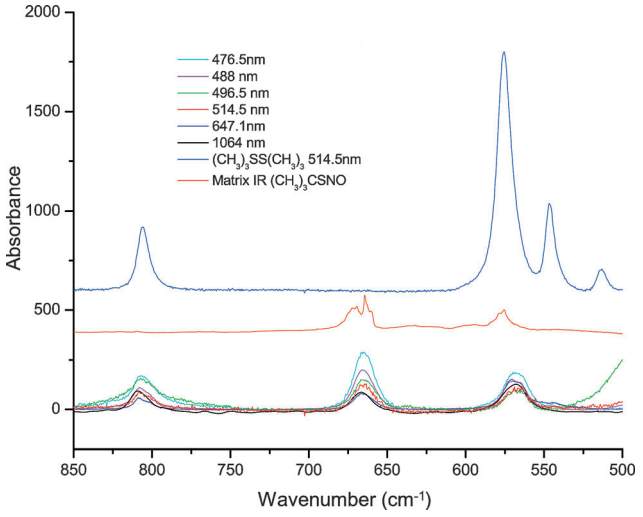

Figure 7. Normalized RR spectra of $(CH_3)_3CSNO$ in the C–C, C–S, and S–N stretching fundamental region. RR spectra of $((CH_3)_3CSSC(CH_3)_3$ and matrix IR spectra of $(CH_3)_3CSNO$ are included for comparison.

Contrasting the liquid Raman and the matrix IR spectra of the title molecule, it becomes apparent that the Raman band at 806 cm^{-1} has no evident counterpart in the IR spectra. This is a clear evidence of a symmetric origin for this vibration. In agreement with the computed values at 853 and 845 cm^{-1} calculated for the *anti* and *syn* rotamers, respectively, using the MP2(full)/cc-pVTZ level of approximation, this band has been assigned to a C–C symmetric vibration. The maximum of Raman activity is again observed when the liquid sample is excited with 476.5 nm radiation. Extreme differences have been reported for the ν(C–S) normal modes of vibration in thionitrites. This mode appears in the gas-phase IR spectrum at 731 cm^{-1} in CH_3SNO and decreases upon fluorine substitution to 442 cm^{-1} in CF_3SNO, and are observed at 781 and 693 cm^{-1} for CF_3CH_2SNO and CH_3CH_2SNO, respectively. The same displacement has been noted also for the S–N stretching vibration. This mode has been reported at 759 cm^{-1} in CF_3SNO, 649 cm^{-1} in CH_3SNO, and was computed at 295 and 398 cm^{-1} for CF_3CH_2SNO and CH_3CH_2SNO, respectively.[19,25]

By comparing the liquid Raman spectra of both samples as depicted in the Figure 7, the vibration appearing at 665 cm^{-1} in the liquid Raman spectra of $(CH_3)_3CSNO$, with its maximum for excitation at 476.5 nm, is not present under the same conditions for the $(CH_3)_3CSSC(CH_3)_3$ sample. Therefore, this band is straightforwardly assigned to the S–N normal stretching vibration of $(CH_3)_3CSNO$. Its computed values are 700 and 686 cm^{-1} for the *syn* and *anti* conformer, respectively. The third intense band in this region appears at 567 cm^{-1} in the liquid Raman spectra. Its relative maximum is again observed upon excitation with the 476.5 nm Ar^+ laser line, and was assigned with confidence to the C–S stretching band, also in good agreement with the computed data (601 and 590 cm^{-1} for the *anti* and *syn* form, respectively).

According to the UV/Vis spectrum depicted in Figure 8, the resonance effect observed in the Raman spectra is related with the structured 350 nm band more than with the 555 or 595 nm UV/Vis bands. In effect, the progression observed in the relative intensity of the resonance Raman spectra is in agreement with a post-resonance effect linked to the 350 nm band. The band centered at 350 nm has a clear vibrational progression with a mean difference of 916 cm^{-1}. For the 260 nm band, the situation is less clear.

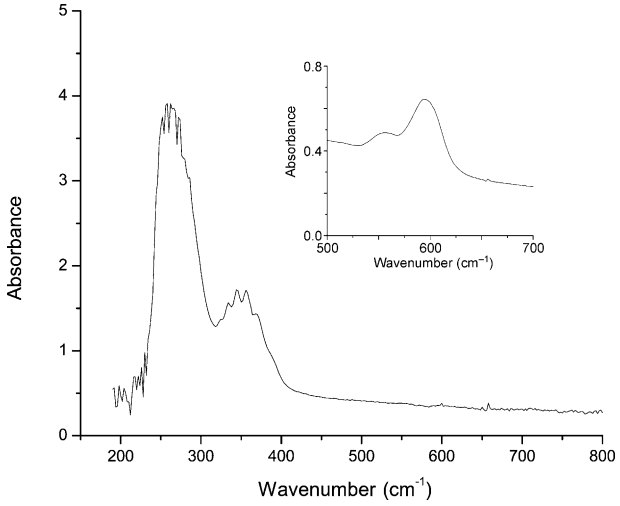

Figure 8. The UV/Vis spectrum of a solution 2×10^{-3} M of $(CH_3)_3CSNO$ in chloroform. The 700–500 nm region has been enlarged in the subsection for a 1×10^{-1} M solution.

In summary, $(CH_3)_3CSNO$ has been isolated and studied using GED, vibrational spectroscopy including gas-phase IR spectroscopy, resonance Raman spectra of the liquid, photochemical matrix studies at cryogenic temperatures, UV/Vis spectra of the solution, and the results were complemented by computed values. The most abundant conformer of $(CH_3)_3CSNO$ is *anti*, while *syn* is less abundant. Both conformers co-exist in equilibrium in the gas phase at ambient temperature and randomize under matrix conditions under UV/Vis broad band irradiation.

Experimental Section

Synthesis, purification, and subsequent manipulation of *tert*-butyl thionitrite were carried out in a glass evacuated system equipped with PTFE stems (Young valves) and greased joints if necessary. The method reported by Tasker and Jones was used.[31] Slightly more than the stoichiometric amount of NOCl was condensed onto 0.01 mol of $(CH_3)_3CSH$ contained in a Carius tube reactor cooled with liquid nitrogen. Then the ampoule was warmed to $-30\,^{\circ}C$ and after a few minutes the reaction was complete. The reaction mixture was distilled and $(CH_3)_3CSNO$ was collected as a bright green liquid in a U-trap cooled at $-45\,^{\circ}C$ while NO, HCl, and residual NOCl were trapped in liquid nitrogen.

Gas-phase electron diffraction was used to determine the gas-phase structure and conformational composition of $(CH_3)_3CSNO$. Experiments were done at Bielefeld University using the GED apparatus described elsewhere.[32] The experimental details are given in the Supporting Information, Table S1. Data reduction and calibration against benzene diffraction patterns, recorded along the experiments, have been performed as described.[33] Structural analyses were performed with the UNEX 1.6 program.[34] All refinements were done using two intensity curves simultaneously (Supporting Information, Figure S2), one from the short and another from the long camera distance, which were obtained by averaging independent intensity curves obtained in experiment. For the definition of independent geometrical parameters and their groups in least-squares refinements see Table 1. The differences between values of parameters in one group were kept fixed at the values taken from MP2(full)/cc-pVTZ calculations. Mean-square amplitudes were refined in groups (Supporting Information, Table S2 and S3). For this purpose, the scale factors (one per group) were used as independent parameters. Thus, the ratios between different amplitudes in one group were fixed on the theoretical values, calculated from B3LYP/6–31G(d,p) quadratic and cubic force fields. The full matrix of correlations between parameters in the least-squares refinement is given in the Supporting Information, Table S6. The experimental and best model molecular intensity curves together with corresponding differences are shown in the Supporting Information, Figure S3.

IR spectra of the vapor sample were recorded at a resolution of 2 cm^{-1} in the range 4000–400 cm^{-1} with a Bruker IFS 66v FTIR instrument.

Raman spectroscopy: 1) A Raman triple grating spectrometer system with a resolution of 2 cm^{-1} and Ar^+ and Kr^+ lasers were used to record liquid Raman spectra of the sample. The same placed in a 4 mm glass capillary was measured using 100 mW of different excitation lines of the laser. 2) FT-Raman spectra were run on liquid $(CH_3)_3CSNO$ with a Bruker RFS 100/S FT Raman spectrometer. The sample placed in a 4 mm glass capillary was measured using 16.5 mW of a 1064 nm Nd:YAG laser (ADLAS, DPY 301, Lübeck, Germany).

Matrix-isolation spectroscopy: A gas mixture of $(CH_3)_3CSNO$ with Ar (AGA) in the relative ratio of ca. 1:560, prepared by standard manometric methods, was deposited on a CsI window cooled to about 10 K by means of a Displex closed-cycle refrigerator (SHI-APD Cryogenics, model DE-202) using the pulse deposition technique at La Plata University.[35] The matrix-isolated FTIR spectra were recorded on a Nexus Nicolet instrument equipped with either an MCTB for the ranges 4000–400 cm^{-1}. Following deposition and IR analysis of the resulting matrix, the sample was exposed to broad-band UV/Vis radiation ($200 \leq \lambda \leq 800$ nm) from a Spectra-Physics Hg-Xe arc lamp operating at 500 W. The output from the lamp was limited by a water filter to absorb IR radiation and so minimize any heating effects. The IR spectra of the matrix with 0.5 and 0.125 cm^{-1} resolution were then recorded at different times of irradiation in order to monitor closely any change in the spectra.

UV/Vis spectra of a solution were recorded using a standard quartz cell placed in the sample compartment of a UV/Vis Hewlett–Packard 8454 A diode array spectrometer (2 nm resolution).

Acknowledgements

The Argentinean authors thank the Consejo Nacional de Investigaciones Científicas y Técnicas (CONICET) (PIP 0352), the Agencia Nacional de Promoción Científica y Tecnológica (ANPCyT), the Comisión de Investigaciones Científicas de la Provincia de Buenos Aires (CIC), and the Facultad de Ciencias Exactas, UNLP for financial support. Furthermore, we acknowledge support by Deutsche Forschungsgemeinschaft (DFG) (international grant MI477/18-1, research stay of A.C., and support for the core facility GED@BI (MI477/21-1).

Keywords: gas-phase electron diffraction · matrix IR spectroscopy · photochemistry · resonance Raman spectroscopy · *S*-nitrosothiols

[1] J. S. Stamler, D. I. Simon, J. A. Osborne, M. E. Mullins, O. Jaraki, T. Michel, D. J. Singel, J. Loscalzo, *Proc. Natl. Acad. Sci. USA* **1992**, *89*, 444–448.
[2] S. Oae, K. Shinhama, *Org. Prep. Proced.* **1983**, *15*, 165–198.
[3] D. Z. Levett, B. O. Fernandez, H. L. Riley, D. S. Martin, K. Mitchell, C. A. Leckstrom, C. Ince, B. J. Whipp, M. G. Mythen, H. E. Montgomery, M. P. Grocott, M. Feelisch, *Sci. Rep.* **2011**, *109*, 1–8.
[4] R. Greenwald, A. M. Fitzpatrick, B. Gaston, N. V. Marozkina, S. Erzurum, W. G. Teague, *PLoS ONE* **2010**, *5*, 1–6.
[5] A. A. Eroy-Reveles, P. K. Mascharak, *Future Med. Chem.* **2009**, *1*, 1497–1507.
[6] U. K. Bandarage, L. Chen, X. Fang, D. S. Garvey, A. Glavin, D. R. Janero, L. G. Letts, G. J. Mercer, J. K. Saha, J. D. Schroeder, M. J. Shumway, S. W. Tam, *J. Med. Chem.* **2000**, *43*, 4005–4016.
[7] M. Hochlaf, R. Linguerri, J. S. Francisco, *J. Chem. Phys.* **2013**, *139*, 234304–234308.
[8] R. K. Szilagyi, D. E. Schwab, *Biochem. Biophys. Res. Commun.* **2005**, *330*, 60–64.
[9] R. M. Romano, C. O. Della Védova, *J. Mol. Struct.* **2000**, *522*, 1–26.
[10] G. E. Carnahan, P. G. Lenhert, R. Ravichandran, *Acta Crystallogr. B* **1978**, *34*, 2645–2648.
[11] N. Arulsamy, D. S. Bohle, J. A. Butt, G. J. Irvine, P. A. Jordan, E. Sagan, *J. Am. Chem. Soc.* **1999**, *121*, 7115–7123.
[12] M. D. Bartberger, K. N. Houk, S. C. Powell, J. D. Mannion, K. Y. Lo, J. S. Stamler, E. J. Toone, *J. Am. Chem. Soc.* **2000**, *122*, 5889–5890.
[13] J. Yi, M. A. Khan, J. Lee, G. B. Richter-Addo, *Nitric Oxide* **2005**, *12*, 261–266.

[14] L. L. Perissinotti, D. A. Estrin, G. Leitus, F. Doctorovich, *J. Am. Chem. Soc.* **2006**, *128*, 2512 – 2513.
[15] M. Marazzi, A. López-Delgado, M. A. Fernández-González, O. Castaño, L. M. Frutos, M. Temprado, *J. Phys. Chem. A* **2012**, *116*, 7039 – 7049.
[16] J. (Banus) Mason, *J. Chem. Soc. A* **1969**, 1587 – 1592.
[17] R. M. Romano, C. O. Della Védova, *J. Mol. Struct.* **1999**, *513*, 85 – 99.
[18] J.-M. Lu, J. M. Wittbrodt, K. Wang, Z. Wen, H. B. Schlegel, P. G. Wang, J.-P. Cheng, *J. Am. Chem. Soc.* **2001**, *123*, 2903 – 2904.
[19] Q. K. Timerghazin, G. H. Peslherbe, A. M. English, *Org. Lett.* **2007**, *9*, 3049 – 3052.
[20] Q. K. Timerghazin, A. M. English, G. H. Peslherbe, *Chem. Phys. Lett.* **2008**, *454*, 24 – 29.
[21] A. Cánneva, C. O. Della Védova, N. W. Mitzel, M. F. Erben, *J. Phys. Chem. A* **2015**, *119*, 1524 – 1533.
[22] R. J. Philippe, H. Moore, *Spectrochim. Acta* **1961**, *17*, 1004 – 1015.
[23] Y. Fu, Y. Mou, B. Lin, Q.-X. Guo, *J. Phys. Chem. A* **2002**, *106*, 12386 – 12392.
[24] L. Field, R. V. Dilts, R. Ravichandran, P. G. Lenhert, G. E. Carnahan, *J. Chem. Soc. Chem. Commun.* **1978**, 249 – 250.
[25] J. Lee, G.-B. Yi, D. R. Powell, M. A. Khan, G. B. Richter-Addo, *Can. J. Chem.* **2001**, *79*, 830 – 840.
[26] K. Goto, Y. Hino, T. Kawashima, M. Kaminaga, E. Yano, G. Yamamoto, N. Takagi, S. Nagase, *Tetrahedron Lett.* **2000**, *41*, 8479 – 8483.
[27] C. O. Della Védova, H.-G. Mack, *Inorg. Chem.* **1993**, *32*, 948 – 950.
[28] T. R. Schaffer, PhD Thesis, Universität Regensburg (Germany), **2005**.
[29] J. S. Stamler, E. J. Toone, *Curr. Opin. Chem. Biol.* **2002**, *6*, 779 – 785.
[30] D. H. Christensen, N. Rastrup-Andersen, D. Jones, P. Klabof, E. R. Lippincott, *Spectrochim. Acta A* **1968**, *24*, 1581 – 1589.
[31] H. S. Tasker, H. O. Jones, *J. Chem. Soc.* **1909**, *95*, 1910 – 1918.
[32] R. J. F. Berger, M. Hoffmann, S. A. Hayes, N. W. Mitzel, *Z. Naturforsch. B* **2009**, *64*, 1259 – 1268.
[33] a) Y. V. Vishnevskiy, *J. Mol. Struct.* **2007**, *833*, 30 – 41; b) Y. V. Vishnevskiy, *J. Mol. Struct.* **2007**, *871*, 24 – 32.
[34] Yu. V. Vishnevskiy, UNEX 1.6 Program, Universität Bielefeld, Bielefeld, (Germany), **2014**.
[35] R. N. Perutz, J. J. Turner, *J. Chem. Soc. Faraday Trans. 2* **1973**, *69*, 452 – 461.

Received: February 27, 2015
Published online on ■■ ■■, 0000

FULL PAPER

Structure Elucidation

*A. Canneva, M. F. Erben, R. M. Romano, Y. V. Vishnevskiy, C. G. Reuter, N. W. Mitzel, C. O. Della Védova**

■■ – ■■

The Structure and Conformation of $(CH_3)_3CSNO$

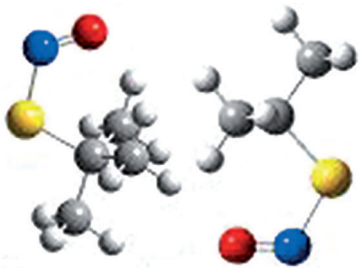

Thionitrite-containing compounds are elusive and thus have been little-characterized and analyzed. The structural, conformational, and spectroscopic characterization of $(CH_3)_3CSNO$ and comparisons with some relevant antecedents were carried out gain an understanding in the biochemical behavior of this family. The first gas-phase electron diffraction study for a RSNO species is also presented.